

Supporting Information

Aluminium-doped cadmium sulfide homojunction photoelectrode with optimal film quality and water-splitting performance

**Jiangwei Zhang^{12#}, Fei Yu^{2#}, He Yu², Shuhui Yang¹³, Gaotian Zhang², Feng Jiang¹,
Menglong Zhang^{2*} and Dongxiang Luo^{1*}**

¹School of Chemistry and Chemical Engineering/Institute of Clean Energy and Materials/Guangzhou Key Laboratory for Clean Energy and Materials/Huangpu Hydrogen Innovation Center, Guangzhou University, Guangzhou 510006, PR China

²Institute of Hydrogen Energy for Carbon Peaking and Carbon Neutralization, School of Semiconductor Science and Technology, South China Normal University, Foshan, 528225, China

³Institut des Nanosciences de Paris (INSP), Faculty of Science&Engineering, Sorbonne University, place Jussieu, Paris, 75005, France

Corresponding author

E-mail address: mlzhang@m.scnu.edu.cn (Menglong Zhang) and luodx@gdut.edu.cn (Dongxiang Luo)

Equations related in this work

1. Theoretical maximum photocurrent density (J_{abs})

Theoretical maximum photocurrent density (J_{abs}) is the photocurrent density assuming that all absorbed photons can be converted into current (i.e., APCE = IPCE/LHE = 100%), it is a constant with the AM 1.5G spectrum and the light harvesting efficiency of the fixed photoelectrode. In the case of J_{abs} , it can be calculated according to the following equation:

$$J_{\text{abs}} = \int_{\lambda_1}^{\lambda_2} \frac{\lambda \times \text{LHE}(\lambda) \times P(\lambda)}{1240} d(\lambda) \quad \text{Eq. S1}$$

S1

where λ and $P(\lambda)$ are the light wavelength (nm) and the corresponding power density ($\text{mW cm}^{-2} \text{ nm}^{-1}$) for the standard solar spectrum AM 1.5G (ASTMG-173-03), respectively. $\text{LHE}(\lambda)$ is light absorption efficiency. The integrated power ($\text{W}\cdot\text{m}^{-2}$) was then divided by 1.23 V vs. RHE to convert it (Figure S6).¹

2. The charge separation efficiency (η_{sep}) and charge injection efficiency (η_{inj})

Photocurrent density arising from PEC water oxidation can be described by the following equation:

$$J_{\text{H}_2\text{O}} = J_{\text{abs}} \times \eta_{\text{sep}} \times \eta_{\text{inj}} \quad \text{Eq. S2}$$

Eq. S2

η_{sep} is the ratio of photogenerated holes which have migrated to the semiconductor/electrolyte interfaces, and η_{inj} is the ratio of photogenerated holes participated in water oxidation reaction. In this work, the widely used $\text{Na}_2\text{S}/\text{Na}_2\text{SO}_3$ was chosen as the hole scavenger.² η_{sep} and η_{inj} were calculated according to the Eq.S3 and Eq. S4, respectively :

$$\eta_{\text{sep}} = \frac{J_{\text{Na}_2\text{S}/\text{Na}_2\text{SO}_3}}{J_{\text{abs}}} \quad \text{Eq. S3}$$

S3

$$\eta_{inj} = \frac{J_{H_2O}}{J_{Na_2S/Na_2SO_3}}$$

Eq.

S4

J_{Na_2S/Na_2SO_3} and J_{H_2O} are the photocurrent densities measured with aqueous (0.25 M $Na_2S/0.35$ M Na_2SO_3 , pH=12.9) and with aqueous (KOH/0.35 M Na_2SO_3 , pH=12.9), respectively (**Figure S7**).

Supplemental Figures

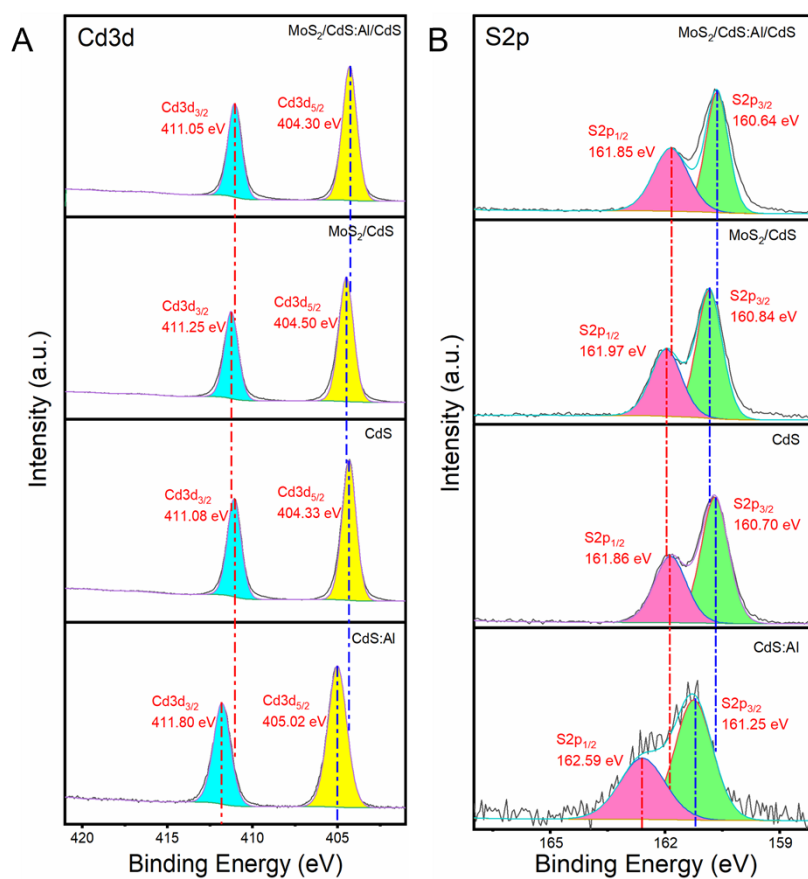


Figure S1. XPS Binding energy of Cd and S in different composition. (A) Cd3d (B) S2p

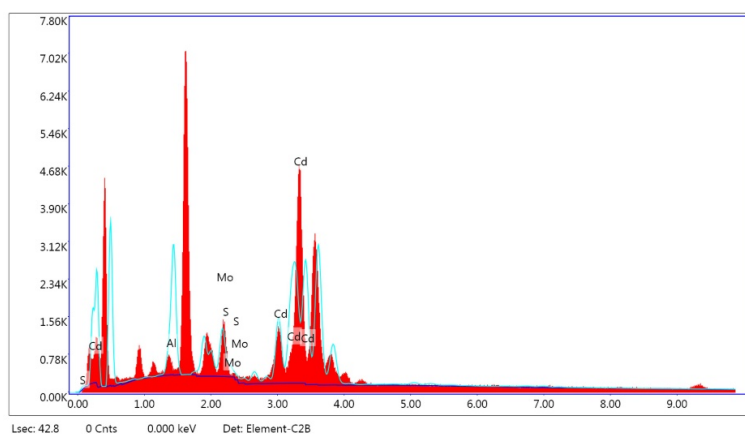


Figure S2. The elemental composition of MoS₂/CdS:Al/CdS electrode analyzed by EDS.

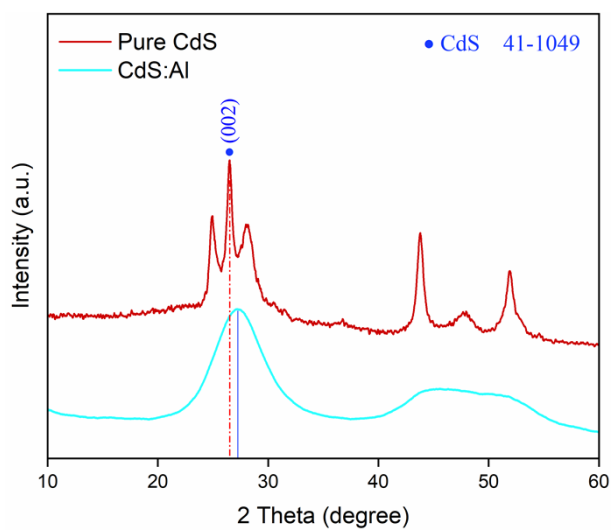
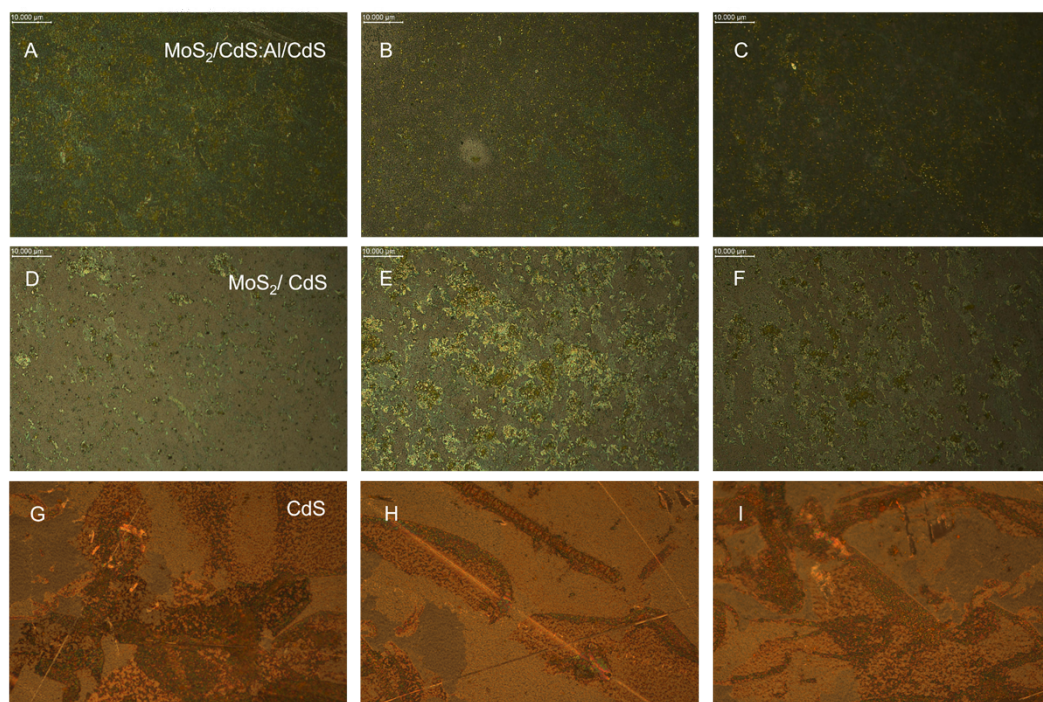


Figure S3. The PXRD patterns of the as-prepared of CdS:Al film.



Figure

re S4. Optical microscope images of (A-C) $\text{MoS}_2/\text{CdS:Al}/\text{CdS}$ films, (D-F) MoS_2/CdS films, (G-I) CdS films at 50 times magnification.

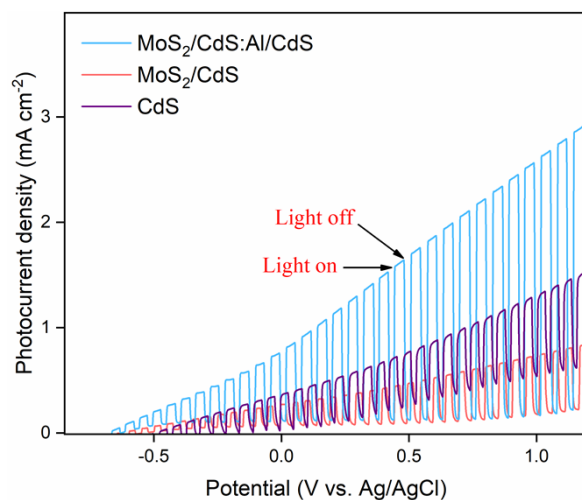


Figure S5. The LSV curves measured of CdS, MoS₂/CdS and MoS₂/CdS:Al/CdS with aqueous (KOH/Na₂SO₃) under chopped illumination.

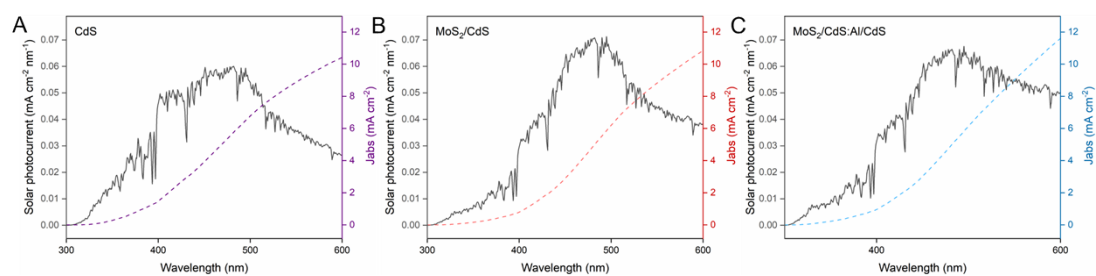


Figure S6. J_{abs} of (A) CdS; (B) MoS₂/CdS; (C) MoS₂/CdS:Al/CdS photoanodes (assuming 100% absorbed photo-to-current conversion efficiency for photons).

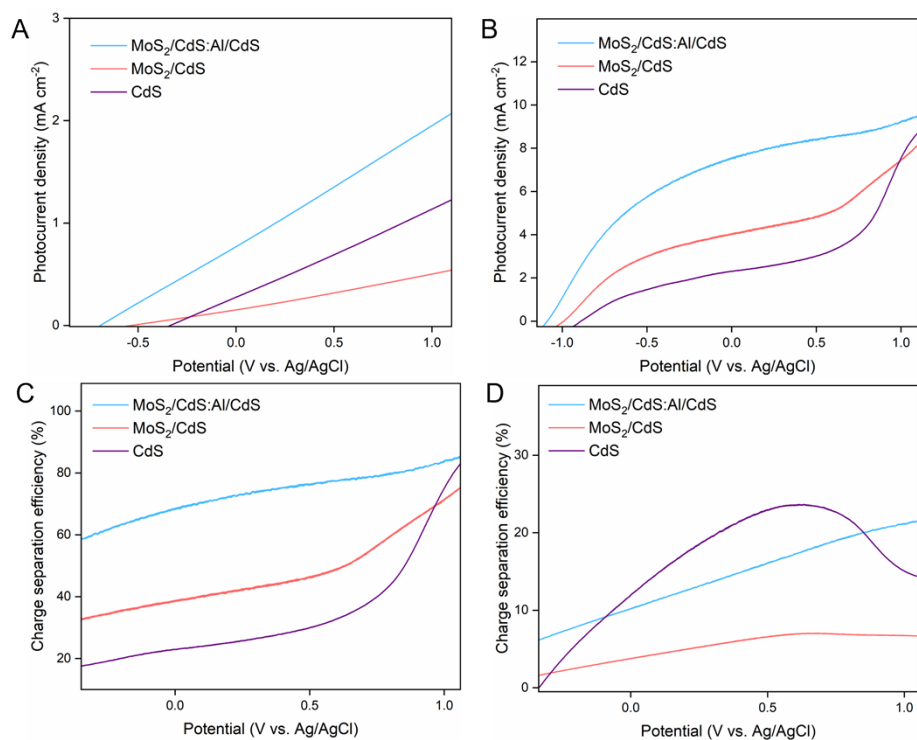


Figure S7. (A) LSV plots measured with aqueous (KOH/Na₂SO₃) and (B) LSV plots measured with aqueous (Na₂S/Na₂SO₃); (C) bulk charge separation efficiency (η_{sep}) and (D) Surface charge injection efficiency (η_{inj}) of the fabricated photoanodes.

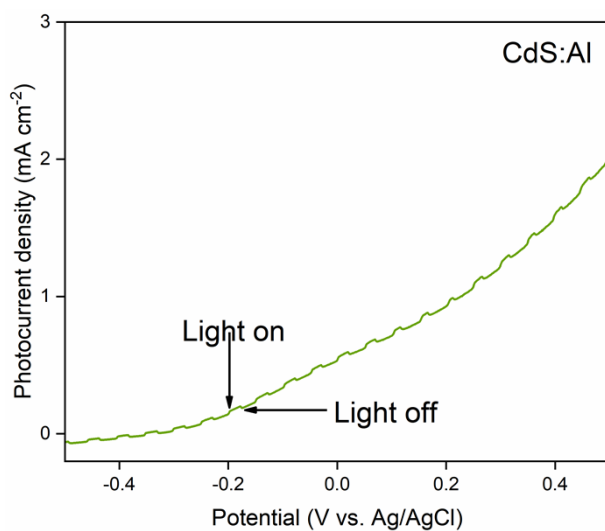


Figure S8. LSV test on CdS:Al film under chopped illumination.

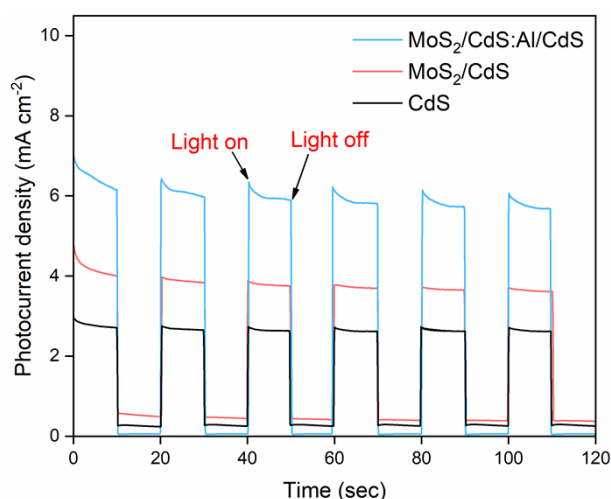


Figure S9. The I-T curves at a constant bias voltage (0.58 V vs. $V_{Ag/AgCl}$) of CdS, MoS₂/CdS and MoS₂/CdS:Al/CdS.

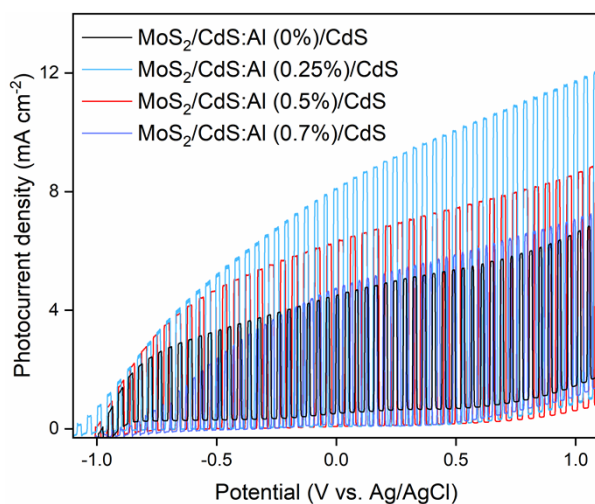


Figure S10. LSV under chopped illumination of the different atomic ratio of Al element in MoS₂/CdS:Al/CdS, all the samples were prepared using 20 SILAR cycles, the default SILAR cycles of the CdS layer and the atomic ratio of Al in CdS:Al layer of MoS₂/CdS:Al/CdS was set as 20 times and 0.25 at%, respectively.

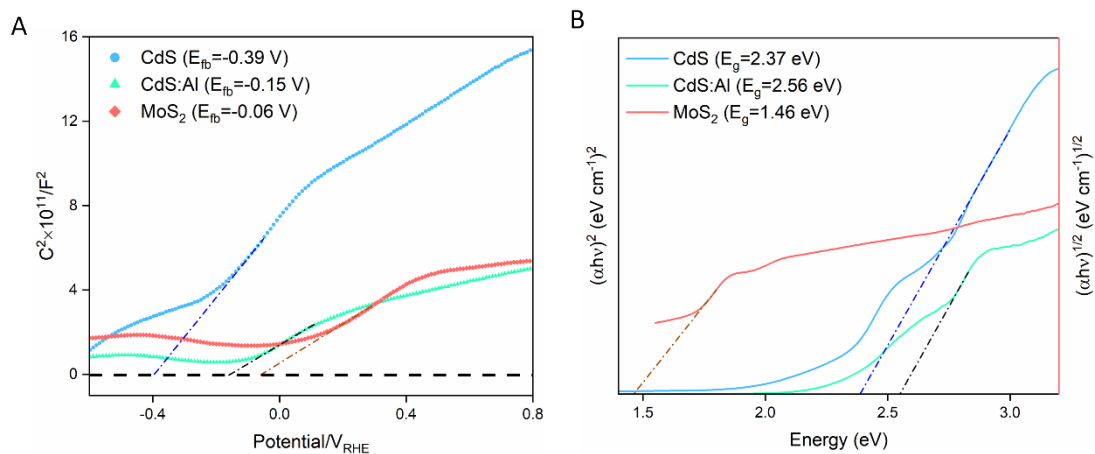


Figure S11. (A) Mott-Schottky plot of CdS, CdS:Al and MoS₂ in darkness; (B) The tauc-plot of CdS, CdS:Al and MoS₂.

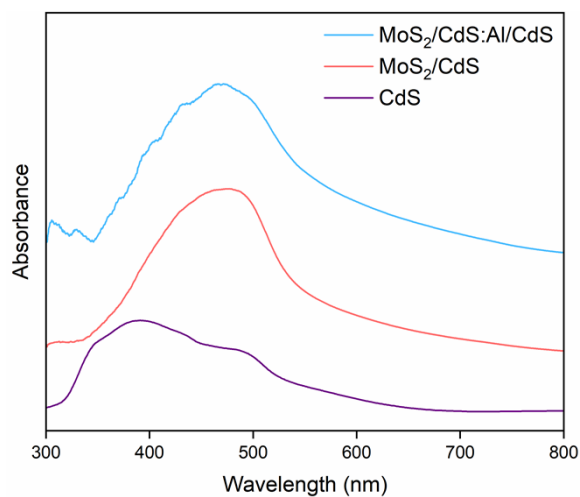


Figure S12. The absorbance spectra of MoS₂/CdS:Al/CdS film, MoS₂/CdS film and CdS film.

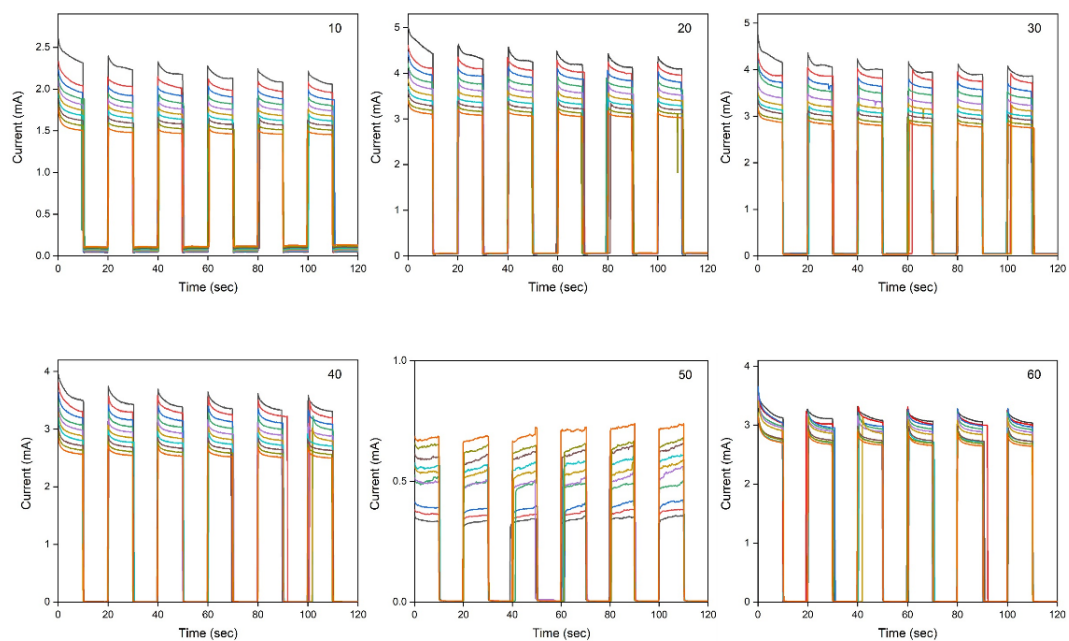


Figure S13. The chronoamperometry tests for 10-60 SILAR cycles over the $\text{MoS}_2/\text{CdS}:\text{Al}/\text{CdS}$ samples.

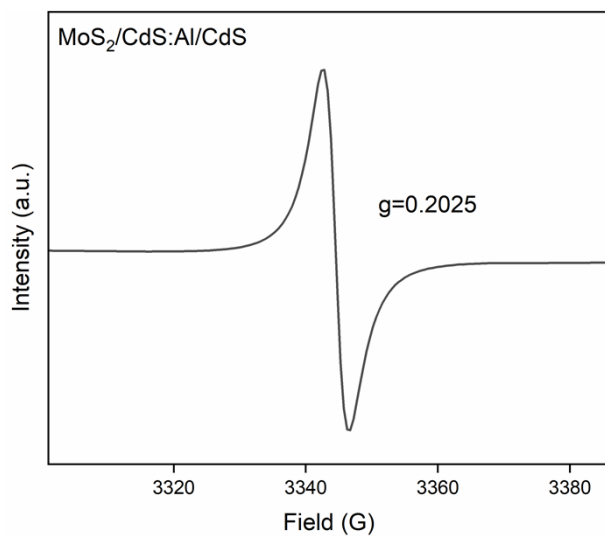


Figure S14. EPR spectra of $\text{MoS}_2/\text{CdS}:\text{Al}/\text{CdS}$ after 5 min illumination.



Video S1. Hydrogen production video of MoS₂/CdS:Al/CdS films.

References

1. L. Li, H. Zhang, C. Liu, P. Liang, N. Mitsuzaki and Z. Chen, *Journal of Materials Science*, 2018, **54**, 659-670.
2. A. Kudo and Y. Miseki, *Chemical Society Reviews*, 2009, **38**, 253-278.